Nitrous oxide emissions from a commercial cornfield (Zea mays) measured using the eddy-covariance technique

Haiyan Huang[1,] Junming Wang[1*], Dafeng Hui[2], David R. Miller[3], Sudeep Bhattarai[2], Sam Dennis[2], David Smart[4], Ted Sammis[5], and K. Chandra Reddy[2]

[1]*Climate Science Section, Illinois State Water Survey, Prairie Research Institute, University of Illinois at Urbana-Champaign, Champaign, IL 61802, USA*

[2]*College of Agriculture, Human and Natural Sciences, Tennessee State University, Nashville, TN 37209, USA.*

[3] *Department of Natural Resources and Environment, University of Connecticut, Storrs, CT 06269, USA.*

[4]*Department of Viticulture and Enology, University of California, Davis, CA 95616, USA.*

[5]*Department of Plant and Environmental Science, New Mexico State University, Las Cruces, NM 88003, USA.*

* *Corresponding author address:* Junming Wang, Climate Science Section, Illinois State Water Survey, Prairie Research Institute, University of Illinois at Urbana-Champaign, 2204 Griffith Dr., IL 61820.

E-mail: wangjim@illinois.edu

ABSTRACT

Increases in observed atmospheric concentrations of the long-lived greenhouse gas, nitrous oxide (N_2O), have been well documented. However, information on event-related instantaneous emissions during fertilizer applications is lacking. With the development of fast-response N_2O analyzers, the eddy covariance (EC) technique can be used to gather instantaneous measurements of N_2O concentrations to quantify the exchange of nitrogen between the soil and atmosphere. The objectives of this study were to evaluate the performance of a new EC system, to measure the N_2O flux with the system, and finally to examine relationships of the N_2O flux with soil temperature, soil moisture, precipitation, and fertilization events. An EC system was assembled with a sonic anemometer and a fast-response N_2O analyzer (quantum cascade laser spectrometer) and applied in a cornfield in Nolensville, Tennessee during the 2012 corn growing season (April 4–August 8). Fertilizer amounts totaling 217 kg N ha^{-1} were applied to the experimental site. Results showed that this N_2O EC system provided reliable N_2O flux measurements. The cumulative emitted N_2O amount for the entire growing season was 6.87 kg N_2O-N ha^{-1}. Seasonal fluxes were highly dependent on soil moisture rather than soil temperature. This study was one of the few experiments that continuously measured instantaneous, high-frequency N_2O

emissions in crop fields over a growing season of more than 100 days.

1. INTRODUCTION

As the largest corn producer in the world, the United States produces about one-third of the world's corn crop (about 84 million ha in 2011) (http://www.epa.gov/agriculture/ag101/cropmajor.html). Corn is a nitrogen- (N) intensive crop. Every year, large amounts of N are applied to cornfields, but its efficiency is low (30% – 59%) (Halvorson et al. 2005). A large proportion of applied N can be leached to groundwater (e.g., NO_3^-) and/or emitted to the atmosphere (e.g., nitrous oxide , N_2O; nitric dioxide , NO; or nitrogen dioxide, NO_2).

N_2O is one of the longest lived greenhouse gases (GHGs) and has an estimated radiative forcing of 0.15 Wm^{-2}, compared to carbon dioxide (CO_2) at 2.43 Wm^{-2} and methane (CH_4) at 0.48 Wm^{-2} (Forster et al. 2007). In addition to its contribution to global warming, N_2O also plays an important role in stratospheric ozone depletion through O (1D) oxidation (Ravishankara et al. 2009). The volume concentration of N_2O in the atmosphere has increased from 273 parts per billion dry air mole fraction (ppbv) in 1950 to 319 ppbv in 2005 (Forster et al. 2007). The major source of anthropogenic N_2O in the atmosphere is believed to be N fertilization accounting for up

67 to 80% of anthropogenic N_2O emissions (Kroeze et al. 1999; Mosier et al. 1998). N_2O emitted
68 from soil is produced by bacterial processes, mainly through nitrification and denitrification
69 (Davidson and Swank 1986). These processes may be affected by several factors, including the
70 percentage of water-filled pore spaces in soil (WFPS) (Dobbie and Smith 2003; Davidson 1991),
71 mineral N concentrations in the soil (Ma et al. 2010; Bouwman et al. 2002; Bouwman 1996),
72 crop type, soil type, soil moisture, air/soil temperature, and oxygen supply within the soil strata.
73 Therefore, N_2O emissions are typically highly variable both in time and space, and are difficult to
74 quantify.

75 Significant efforts have been invested in developing reliable tools for measuring
76 instantaneous N_2O emissions from soil to the atmosphere. The two major measurement methods
77 currently available for N_2O fluxes are the chamber method and the eddy covariance (EC) method
78 (Denmead 2008; Molodovskaya et al. 2011). The chambers, either closed (static) or open
79 (dynamic flow), are the traditional tools that have been used in different land management
80 systems (farmland, forest, and grassland) (Tao et al. 2013; Liu et al. 2012; Arnolda et al. 2005;
81 Klemedtsson et al. 1996). The chamber method is simple in concept and operation, as well as
82 low in cost. However, several limitations may affect the data quality, such as small area
83 coverage, called the footprint, (≤ 1 m^2), disturbance of the soil environment, and low sampling
84 frequency (Molodovskaya et al. 2011; Denmead 2008). The EC method calculates the spatial
85 averaged flux from a larger "field scale footprint (10 m^2 $\sim$ 1 km^2) (Denmead 2008). Unlike the
86 chamber method, the EC method does not disturb the soil and crop ecosystem and provides a
87 continuous and real-time flux measurement.

88 The EC method is based on the Reynolds decomposition theory that a turbulent variable (x) can
89 be represented by a time-averaged component ($\bar{x}$) and a fluctuation component (x') (e.g.,

Famulari et al. 2010; Kaimal and Finnigan 1994; Stull 1988):

$$x = \bar{x} + x' \quad . \tag{1}$$

In the EC method, the vertical flux of a gas is expressed as the covariance between the vertical wind velocity and gas concentration:

$$J = \overline{w'c'} \tag{2}$$

where J is the gas vertical flux, w' and c' are the deviations of vertical wind velocity (w) and gas concentration (c), respectively, and the overbar represents a time average. The EC method requires rapid, simultaneous (or near- simultaneous) measurements of gas concentration and wind velocity at the same point in space. With the developments of fast-response N_2O analyzers in recent years, the EC method has become more common (Jones et al. 2011; Mammarella et al. 2010; Eugster et al. 2007; Pihlatie et al. 2005; Di Marco et al. 2004; Edwards et al. 2003). In this project, an EC system for N_2O measurement was assembled in a commercial cornfield in Nolensville (TN) with a newly available fast-response N_2O analyzer. It was a quantum cascade laser (QCL) spectrometer (model CW-QC-TILDAS-76-CS, Aerodyne Research Inc., Billerica MA).

The objectives of this study were to evaluate the performance of the new N_2O spectrometer in the EC system, to measure the N_2O flux with the system, and finally to examine relationships between the N_2O flux and soil temperature, soil moisture, precipitation, and fertilization events.

2. MATERIALS AND METHODS

2.1. Site description

112 The experimental site was located in a commercial cornfield in Nolensville, Tennessee, 35 km
113 south of Nashville (Figure 1). The field was 300 m (east-west) by 500 m (south-north) with a 2%
114 slope facing west. The soil type was Talbott silty clay loam (fine, mixed, semi-active, thermic
115 Typic Hapludalfs; 32.5% sand, 53.8% silt, 13.8% clay)
116 (http://websoilsurvey.nrcs.usda.gov/app/WebSoilSurvey.aspx). Soybeans were planted in the
117 previous year's rotation. Corn seeds (Roundup Ready BT Hybrid Corn, P1412 HR, Pioneer Hi-
118 Bred International Inc., Johnston, IA) were sown on April 9, 2012. Measurements were
119 continuous from April 4 to August 8, 2012, covering the entire corn-growing season.

120 The agricultural practice was no-till. A weather station (Vantage PRO2 Plus, Davis
121 Instruments, Vernon Hills, IL) was used to record 30-min precipitation, temperature, pressure,
122 wind speed and direction, relative humidity (RH), and solar radiation. The prevailing wind
123 direction was from the southwest during the growing season.

124

125 *2.2. The EC instruments*

126 A sonic anemometer (CSAT3-A, Campbell Sci, Logan, UT) located in the middle of the field
127 measured three-dimensional wind velocities and virtual air temperatures at a sampling rate of 10
128 Hz. It was positioned 1.3 m above the canopy, and was raised as the corn plants grew taller. N_2O
129 concentrations were measured by a quantum cascade laser (QCL) spectrometer (model CW-QC-
130 TILDAS-76-CS, Aerodyne Research Inc., Billerica, MA). The N_2O analyzer was housed in a
131 trailer where a stable working temperature (293-303 K) was maintained. The pressure of the
132 spectrometer sample cell was 4 kpa (30 Torr). The laser was operated at a wave number of 2193
133 cm^{-1}.

The N_2O analyzer was located 50 m from the sonic anemometer. Following the specifications of Eugster et al. (2007), a sampling Teflon tube (6 mm inner diameter, 50 m length) was used to sample the air at the EC sonic anemometer location in the middle of the field and was connected to the N_2O analyzer. The tube intake was 20 cm from the sonic anemometer. Sample air was drawn into the tube intake at a rate of 14 STD L min^{-1}. The analyzer provided 10 Hz measurements of N_2O and water vapor (H_2O) concentrations. The analyzer automatically corrected the H_2O effects on N_2O measurements (WPL and cross-sensitivity of H_2O on N_2O) in real time (Nelson 2002). A Campbell Scientific CR3000 data logger was used to record all the data collected at 10 Hz. The EC measurement footprint ranged from 25 to 90 m upwind, and was calculated using the software EddyPro (version 3.0, LI-COR Biosciences, Lincoln, NE). Soil moisture and soil temperatures were measured with a water content reflectometer (CS616) and an averaging soil thermocouple probe (TCAV, Campbell Sci, Logan, UT), which were buried vertically at a depth of 0-10 cm underground. The mineral NO_3^- and NH_4^+ concentrations in the top 10 cm of soil were measured using a Lachat Flow Injection Auto-analyzer (Loveland, CO). (The Auto-analyzer mixes the sample (liquid state) homogeneously with reagents; the sample and reagents are merged to form a concentration gradient that yields analysis results.)

2.3. N_2O flux calculation and data corrections

The EddyPro version 3.0 was used to process and correct the N_2O flux. EC fluxes were calculated as the covariance of the vertical wind velocity and N_2O concentration over an averaging period:

$$J_{N_2O} = \overline{w' c'_{N_2O}} \times \frac{\rho_a}{M_a} \times 3600 \times 28 \times 10^3 \quad , \qquad (3)$$

where J_{N_2O} is the N_2O flux (μg N_2O-N m^{-2} hr^{-1}), c_{N_2O} is the N_2O concentration in air (ppbv), the component prime ($'$) indicates a deviation from the mean, and the overbar denotes a time average, ρ_a is the density of air (kg m^{-3}) and M_a is the molar mass of air (0.028965 kg mol^{-1}), 3600 represents 3600 seconds per hour, and 28 is the molar mass of two N atoms in N_2O (g $mole^{-1}$).

The averaging period to determine eddy fluxes must be sufficient to adequately sample all the motions that contribute to the fluxes, but an overly long averaging period might affect measurements with irrelevant signals. According to Moncrieff et al. (2004), an averaging period of 30 to 60 minutes is appropriate for gas flux calculations. In this study, a commonly used averaging period of 30 minutes was chosen (Mammarella et al. 2010; Eugster et al. 2007; Aubinet et al. 2000).

EC measurements need several corrections before and after performing a flux calculation. Data spikes can be caused by random electronic spikes in the measuring or recording systems. The de-spike procedure was applied to the raw data (10 Hz) before the calculation of flux. The spike detection and removal method used in this study was similar to that of Vickers and Mahrt (1997). A spike was identified as up to 3 consecutive outliers with respect to a plausible range within a certain time range, and the spike was replaced with the linear interpolation between adjacent data points. The rationale is that if more consecutive values are found to exceed the plausibility threshold, they might be a sign of an unusual yet physical trend (not an outlier). The threshold was set to 3 to 8 times the standard deviation for a given averaging period (3 times for wind velocity and air temperature, and 8 times for N_2O concentrations; these parameters represent the default values in EddyPro).

176 The vertical axis of the sonic anemometer was not always aligned with the local normal to the
177 surface. Therefore, there could be cross-contamination among components of the flux divergence.
178 In order to avoid cross-contamination, an axis rotation was necessary. The EddyPro used a
179 double rotation scheme, in which the u-component was aligned with a local streamline for each
180 30-min interval, and the v-component and w-component were forced to be zero on average.

181 The physical separation of the sonic anemometer and the N_2O analyzer caused a time lag (τ)
182 between the sonic data and N_2O data. Compensation for τ before the covariance calculation is
183 required in the EC technique. In this study, the τ for each 30-min averaging period was obtained
184 by searching for the maximum cross covariance between sonic variables and analyzer
185 measurements.

186 All EC systems applied to trace gas measurements tend to underestimate the true atmospheric
187 fluxes due to physical limitations of the instruments which cause flux losses at high (e.g.,
188 damping effects from long intake tube) and low frequencies. The commonly used methods of
189 addressing spectral attenuation have been described (e.g., Ferrara et al., 2012, and Moncrieff et al.
190 2004). The EddyPro software program provides several options for spectral correction. In this
191 study at the low frequency range, the analytic correction proposed by Moncrieff et al. (2004) was
192 used, and at the high frequency range, the spectral loss was corrected following Ibrom et al.
193 (2007) and Horst and Lenschow (2009).

194 The frequency loss ratio ($\frac{\Delta\emptyset}{\emptyset}$) was calculated as:

195 $$\frac{\Delta\emptyset}{\emptyset} = 1 - \frac{\int_0^{+\infty} CO_M df}{\int_0^{+\infty} CO_T df} \quad (4)$$

where the CO_T is the theoretical N_2O flux cospectrum following Kaimal et al. (1972), CO_M is the N_2O flux cospectra from the measured data, and f is the spectral frequency.

The EddyPro software outputs a frequency correction factor for N_2O (N_2O-cf) as the ratio of the frequency-corrected flux divided by the flux before the frequency correction. Therefore the frequency correction ratio by EddyPro ($\frac{\Delta\emptyset}{\emptyset}(EP)$) is:

$$\frac{\Delta\emptyset}{\emptyset}(EP) = 1 - \frac{1}{N_2O-cf} \quad (5)$$

2.4. Data for weak turbulence and precipitation conditions

It has been found that under weak wind conditions with no surface heating, turbulence may not develop. Friction velocity (u_*) was used to measure the turbulent state of the atmosphere:

$$u_* = (\overline{\omega' u'^2} + \overline{\omega' v'^2})^{\frac{1}{4}}, \quad (6)$$

where u' and v' are the fluctuations in horizontal downwind and crosswind components.

The determination of an adequate u_* threshold for sufficient turbulent mixing was crucial. The common method to determine the u_* threshold is to examine the scatter plot of night time flux versus u_*, and the threshold is located at the point in which the flux begins to level off as u_* increases (Gu et al. 2005). There are also many statistic-based algorithms used to determine u_* thresholds (Papale et al. 2006; Gu et al. 2005; Saleska et al. 2003). Mammarella (2010) summarizes the appropriate range of the u_* threshold as 0.1 for grassland to 0.3 for forest. In this

study we used 0.2 as the threshold for the cornfield. A u_* threshold value (0.15 m s^{-1}) was obtained using the method in Barr et al., 2012. That value was similar to and slightly smaller than our threshold value of 0.2 m s^{-1}. Therefore, our data processing using 0.2 m s^{-1} threshold value was conservative and warranted to exclude all the low-turbulence data and even excluded some data just around the low- to normal-turbulence transition zone (u_* from 0.15 to 0.2 m s^{-1}). During precipitation conditions, the sonic anemometer sensor heads could be wet, causing errors in the instantaneous measurements. Therefore in this study the N_2O flux data were excluded in low turbulence, $u_* < 0.2$ m s^{-1}, and during rainfall.

2.5 Measurement periods

As noted above, continuous measurements were carried out from April 4 to August 8, 2012. The corn was harvested one week after the study period ended. On August 8, the moisture content of the kernels was less than 25%; therefore the study period covered the entire growing season. Prior to planting and before the EC measurements were initiated, chicken litter (99 kg N ha^{-1}) was applied to the field on March 10. Two applications of fertilizers were subsequently supplied on April 10 (URAN-32-0-0 liquid nitrogen, 39 kg N ha^{-1}) and May 14 (URAN-32-0-0 liquid nitrogen, 79 kg N ha^{-1}). The experimental period was divided into four specific periods based on fertilization or precipitation events (Table 1). The first period started 24 days after the application of chicken litter, and the first liquid fertilizer application (URAN-32-0-0, at a rate of 39 kg ha^{-1}) was within this period. The second period was characterized by the second fertilizer application and high precipitation. The third period was without fertilization and significant precipitation, and the fourth period had high relative precipitation but no fertilization. The data were further divided into two groups according to the measurement time: daytime (7 a.m. to 7 p.m.) and night

time (7 p.m. to 7 a.m.). Mean and standard deviations of the N_2O flux, soil moisture, and soil temperature were obtained and regression and correlation analysis were conducted for day and night for different temporal periods. In the regression analysis, soil moisture and temperature were independent variables and N2O flux was the dependent variable. The regression equations were used for filling gaps at the missing data points. The N_2O flux was then integrated for the whole season to obtain the overall N_2O emission.

3. RESULTS

3.1 The performance of the N_2O analyzer

The precision of the N_2O concentration measurements was characterized under field sampling conditions by the Allan variance technique (Figure 2). In the log-log plot, the measurement variance decreased with the integration time (t) with a slope of -1 when $t \leq 10$ s, indicating that there were no correlations between noise sources (pink noise) at time scales of 0.1 to 10 s. The variance had a broad minimum between 10 and 100 s with a minimum corresponding to 0.006 ppbv of standard deviation. The standard deviation was 0.066 ppbv for 10 Hz (integration time 0.1 s), 0.020 ppbv for 1 Hz (integration time 1 s), and 0.006 ppbv for 0.1 Hz (integration time 10 s).

Figure 3 shows the frequency distribution of time lags during the experimental period. The peak value of the distribution appeared at τ = 6.3 s, which represents the air flow time in the sampling tube between the field collection location and the QCL N_2O analyzer.

257 Figure 4 shows sample cospectra of sensible heat and N_2O and the theoretical N_2O
258 cospectra obtained during a windy day (Figure 4.a) and a windy night (Figure 4.b). A rather good
259 performance of the N_2O cospectrum in the low frequencies was demonstrated. The N_2O
260 cospectrum fell off faster at higher frequencies than the theoretical cospectrum and the sensible
261 heat cospectrum. The N_2O flux frequency loss ratios during the daytime and night time were low
262 (1% and 2%). The frequency correction ratios by EddyPro for the daytime and night time were 18
263 and 19%, respectively.

264 Table 2 shows the variation of the frequency loss ratio of N_2O flux under weak to strong
265 wind conditions (u^* is linearly related to wind speed). In general, the mean of flux frequency loss
266 ratios (including all ratios: ≥0 and <0) increased with increased wind speed (u_*) when $u_* \geq 0.2$ m
267 s^{-1}. When $u_* \leq 0.2$ m s^{-1}, the eddies may not have been well enough developed for the
268 measurements to be accurate. Under the night time condition, the frequency loss ratio was larger
269 than under the daytime condition when the u_* values were in the same category. The average
270 EddyPro frequency correction ratio was 15% to 18%.

271 *3.2 Seasonal variations*

272 A total of 5,197 30-min data points were collected. After applying the two filters ($u_* \geq 0.2$,
273 precipitation free), 1,390 data points remained. In general, the concentration and the flux of N_2O
274 had higher values during and after the fertilizer application but gradually decreased with time, as
275 shown in Figure 5 and Figure 6. However, rainfall (soil moisture) was a trigger for N_2O
276 emissions, which is the reason the flux reached peak values on the day of the largest application
277 of URAN-32-0-0 (May 14), and the lack of peak values of N_2O flux just after the first application

with no rainfall. The growing season was characterized by a number of precipitation events which appeared to increase the N_2O concentration as well as the N_2O flux.

Note the two general seasonal concentration levels in Figure 6. One was before a continuous corn canopy was established in early June, and the second, a continuous canopy that extended from mid-June to August 8. These differences may have been caused by the high applications of the fertilizer and less nitrogen use by the establishing crop before June which resulted in higher soil N availability and more N_2O emissions during that period as shown in Figure 5.

3.3 Diurnal variations

Diurnal variations of the N_2O flux were detected (Figures 7 and 8). Figure 7 contains nearly complete diurnal data for each day for five selected days (>20 hours data per day and $u_* \geq 0.2$ m s^{-1}). The peak flux commonly appeared during the daytime, whereas the flux was low at night except for the third sub-period in Figure 8 when soil moisture was high during the night time. The average daytime and night time N_2O fluxes during the five days were 96.4 ± 11.7 μg N_2O-N m^{-2} hr^{-1} and 59.0 ± 13.0 μg N_2O-N m^{-2} hr^{-1}, respectively. The average flux was about 63% higher during the daytime than during the night time (Figure 7). The average daytime and night time N_2O fluxes during the whole season were 278.8 ± 47.5 and 99.9 ± 29.8 μg N_2O-N m^{-2} hr^{-1}, respectively (All the 'mean $\pm$ number' in this paper are 95% confidence intervals unless otherwise noted). This diurnal response was most likely a temperature response.

3.4 Result statistics

299 The N_2O concentrations and fluxes were highly variable with time. The concentration was 322.8
300 $\pm$ 0.3 ppbv with a coefficient of variation (CV) of 1.24%. The N_2O flux ranged from 0.0 to
301 event-related emissions as high as 11,100 μg N2O-N m^{-2} hr^{-1} with a CV of 317.6% and a mean of
302 257.5 $\pm$ 42.9 μg N_2O-N m^{-2} hr^{-1}. As shown in Table 3, nearly 90% of the data were obtained
303 during the daytime. Fluxes were higher during the daytime than during the night (Table 3 and
304 Figure 7). For the whole experimental period, the total emission was 6.87 kg N_2O-N ha^{-1} (Figure
305 9).

306

307 *3.5 Effects of soil moisture, temperature, and N availability on N_2O emissions*

308 Figure 10 presents an overview of the measured concentration and flux for the whole
309 experimental period, together with soil temperature and soil moisture. Generally, the variations of
310 N_2O concentration and flux followed most closely the pattern of variation of soil moisture. As
311 expected, concentrations and fluxes were usually elevated immediately after precipitation events.
312 As shown in Table 1, there was no fertilization event or significant precipitation in the third
313 period, and thus the N_2O flux was constantly low.

314 In previous studies it has been difficult to generalize and interpret the relationships of N_2O
315 emissions with soil temperature or soil moisture quantitatively because in each specific study the
316 determinants are different. In this study, for the entire experimental period, the N_2O flux was
317 positively correlated to soil moisture with a Pearson correlation coefficient r of 0.42 ($p < 0.001$),
318 while the correlation with soil temperature was poor ($r = -0.079$, $p = 0.003$). Table 4 shows the
319 Pearson correlation coefficients for the periods defined in Table 1. The N_2O flux was significantly
320 correlated with soil moisture except for S1N, which was probably limited by the small sample

size. These correlations indicate that on this site the dominant driver of N_2O emissions was soil moisture in addition to substrate N availability.

Although the soil temperature did not positively correlate to the seasonal N_2O emission, it was significantly and positively correlated to the diurnal (hourly) N_2O emission during the first and second sub-periods (correlation coefficient r_{st}=0.76 and 0.56, $p<0.001$) when soil moisture was not strongly predictive ($r_{sm}<0.36$, $p>0.05$) (Figure 8). Therefore, the peak flux during these sub-periods appeared most often during the day when the soil temperature was relatively high compared to the night. However, during times of significant effects of soil moisture ($r_{sm}>0.45$, $p<0.05$) during the third and fourth sub-periods, the temperature effects on the N_2O flux was not significant ($r_{st}<0.2$, $p>0.05$).

Several studies have found that N_2O flux increased exponentially with soil temperature (Dinsmore et al. 2009; Schindlbacher et al. 2004; Smith et al. 2003). At first we regressed the observed N_2O flux with soil temperature and soil moisture following the exponential functions given by Luo et al. (2013). However, for some periods the coefficients of determination (R^2) were low (< 0.4). Then we regressed the N_2O flux with soil temperature and soil moisture using exponential or polynomial functions (Table 5). The values of R^2 ranged from 0.45 to 0.70. For most of the periods, soil moisture explained a significant amount of the variation in N_2O emissions.

N availability was an important factor in N_2O emissions. The fertilizer amount of the second application was more than twice that of the first application; the large amount of fertilizer provided sufficient N. The volume concentration of NO_3^- in the top 10 cm of soil was 5.5 parts per million (ppmv) on April 15, and was 8.5 ppmv on May 16. The concentrations of NH_4^+ were

16 ppmv and 19.5 ppmv for these two days, respectively. The higher mineral N concentration most likely contributed to the dramatic increase in N_2O concentration and flux after the second application.

4. DISCUSSION

4.1. N_2O analyzer performance

Several studies have been performed for N_2O measurements using QCL spectrometers over grassland or forest (Neftel et al. 2010, 2007; Eugster et al. 2007; Kroon et al. 2007; Nelson et al. 2004). Besides experimental locations, seasons, and/or crop types, the instruments utilized in these studies differed from each other in terms of absorption line and precision. For example, in the studies of Kroon et al. (2007) and Neftel et al. (2010), N_2O was measured at wavelengths of 1271.1 cm^{-1} and 1275.5 cm^{-1}, respectively, while in Neftel et al. (2007) and Eugster et al. (2007), N_2O was measured at 2241.0 cm^{-1} and 2243.1 cm^{-1}, respectively. The precision of the instruments in these four studies, at a sampling rate of 1 Hz, was 0.5, 0.7, 0.3, and 0.3 ppbv, respectively. In our study, the precision was 0.02 ppbv at 1 Hz.

The detection limits of the EC flux were calculated as the standard deviations of the cross covariances between vertical wind fluctuations and gas concentration fluctuations far outside of the true time lag ($-200\ s \le \tau \le -50\ s$, and $50\ s \le \tau \le 200\ s$) (Neftel et al., 2010, Wienhold et al., 1995). Thus the EC detection limits derived from this method was not a constant value and was dependent on the instruments and atmospheric conditions. The mean detection limit in this study was 7.56 ug N m^{-2} hr^{-1}, which was less than half of the N_2O flux detection limit of 17.13 ug N m^{-2} hr^{-1} as reported in Neftel et al. (2010) and 21.60 ug N m^{-2} hr^{-1} in Kroon et al. (2007).

365 It has been shown that the sensible heat cospectrum calculated from sonic temperatures
366 experiences almost no damping (Neftel et al. 2010; Kroon et al. 2007) (Figure 4.a and 4.b).
367 Therefore, an empirical correction approach can be used, based on a comparison of the sensible
368 heat cospectrum and N_2O cospectrum to correct the high frequency loss (Neftel et al. 2010; Kroon
369 et al. 2007).

370 Neftel et al. (2010), under a wind speed of 0.8 to 2 m s^{-1}, reported a 14 to 30% frequency
371 loss correction ratio compared to a mean correction ratio of 16% by EddyPro in this study
372 (corresponding to u_* =0.2 to 0.5 m s^{-1}). Neftel et al. (2010) used vapor cospectra to correct the
373 frequency loss, whereas, this study used the methods in Ibrom et al. (2007), Horst and Lenschow
374 (2009), and Moncrieff et al. (2004), which may account for the difference in frequency loss
375 correction ratios.

376 About 93% of the valid data ($u_* \geq 0.2$ m s^{-1}) in this study were under wind conditions of
377 0.4 m $s^{-1} > u_* \geq 0.2$ m s^{-1} and were in the daytime, when the corresponding mean frequency loss
378 ratio was low, between 2% and 4%. Therefore, the flux may have been overestimated because the
379 mean frequency correction ratio was 16-18% (Table 2).

380 The mean of the positive frequency loss ratios was greater than 22% and the mean of the
381 negative loss ratios was smaller than -37% (for $u_* \geq 0.2$ m s^{-1}) (Table 2). The negative and the
382 positive ratios cancelled out each other and resulted in the mean 2% to 4% frequency loss ratios.
383 Therefore, for long-term N_2O flux measurements, the mean frequency loss may be low.

384 *4.2. N_2O emission compared with the literature*

A number of studies have been carried out to investigate N_2O emissions from soil to the atmosphere, and the results reported in the literature show tremendous variation (Table 6). Previous studies have shown that the N_2O emission depends on several factors, including precipitation, fertilization, tillage, crop type, soil factor, and instrumentation (Ussiri et al. 2009; Wagner-Riddle et al. 2007). Fertilizer application was a prime factor causing a different N_2O emission in previous studies. Generally, the measured flux and cumulative emission were larger with a larger amount of fertilizer application (Table 6). In order to obtain a gross synthesization of these previous studies, shown in Table 6, and how this study fits into them, we plotted those which reported both fertilizer applied and the integrated amount of N_2O emissions. Figure 11 presents a simple linear plot of emissions (Kg N_2O-N Ha^{-1}) (Table 6, column 9) as a function of fertilizer applied (Kg N Ha^{-1}) (Table 6, column 6). The graph demonstrates a general linear trend (R^2=0.48, $p<0.001$) of increasing emissions with increased amounts of N fertilizer, without regard to soil moisture, crop type, tillage, crop management, measurement techniques, or length of time of the study. The simple linear regression shows the ratio of N_2O emissions to N fertilizer to be 0.0143. Thus, in general, it appears that 1.43% of each unit of N fertilizer applied is emitted to the atmosphere as N_2O.

Corn crops were reported in nine of the studies listed in Table 6. They fit the trends described above. Similar amounts of fertilizers were applied in Lee et al. (2009) and Laville et al. (1999) as in this study; and similar orders of N_2O emission were observed in all three. Where lower applications of fertilizer were reported for corn fields (Molodovskaya et al. 2011, Phillips et al. 2009, Ussiri et al. 2009, Wagner-Riddle et al. 2007, and Grant and Pattey 2003), lower N_2O emissions were measured.

In addition to fertilization, tillage also has played a role in governing N_2O emissions. Lee and colleagues (Lee et al. 2009) showed that with the same amounts of fertilizers for corn, sunflower, and chickpea, different tillage could cause differences in N_2O emissions. And fully tilled fields tended to release less N_2O.

In general, forest N_2O emissions have been lower than those from agriculture, which was probably due to the large amount of fertilizers applied to farmland. For example, compared to the flux rate 257.5 ±42.9 μg N_2O-N m^{-2} hr^{-1} in this study, Mammarella et al. (2010) measured an averaged flux of ~10 μg N_2O-N m^{-2} hr^{-1} during May 2 to June 5, 2003 in a beech forest of Denmark. They showed ~ 5 μg N_2O-N m^{-2} hr^{-1} flux during the spring of 2007 in a forest with pine, small-sized spruce, and birch in southern Finland, using both the EC and chamber methods. Eugster et al. (2007) measured N_2O from a forest mixed with beech and spruce using the EC method. The reported flux was 22.4±11.2 μg N_2O-N m^{-2} hr^{-1}.

4.3 Effects of soil moisture, temperature, and N availability on N emissions

Soil moisture is a major factor for N_2O emissions (Table 4). As indicated by Dobbie and Smith (2003) and Davidson (1991), N_2O emitted from soil is caused principally by the microbial nitrogen transformations during both nitrification and denitrification. These processes are closely related to WFPS since denitrification is an anaerobic process, which depends on the balance between the amount of water entering and leaving the soil. Several studies have confirmed that there are connections between increased N_2O emissions and precipitation (Zona et al. 2011; Jungkunst et al. 2008; Neftel et al. 2007, e.g.). In this study, after the first application of fertilizer, precipitation did not occur immediately and there was no significant change in N_2O flux. On the

429 day of the second application, the total precipitation was 3.02 mm and peak values of N_2O fluxes
430 occurred immediately after the precipitation event (Figure 5). The difference of N_2O emission
431 response after first and second applications of fertilizer showed the trigger effect of precipitation on the
432 N_2O emission. The other notable feature of Figure 5 was the remarkable increases of N_2O for the days with
433 precipitation. The variations in the increases may have been mainly caused by the changes in soil moisture
434 content due to precipitation.
435
436 During the whole season, soil temperature was not positively correlated to N_2O flux ($r=-0.084$,
437 $p<0.01$). Apparently soil temperature generally increased with time during the season, while the
438 N_2O flux did not. Therefore the N_2O flux was correlated mainly with soil moisture (Figure 10
439 and Table 4). Thus compared to the factor of soil moisture, soil temperature had rather weak
440 effects on N_2O emissions at this specific site (Table 4).
441 However, when looking at the diurnal cycles, when soil moisture was not a predominant factor ($r_{sm}<$
442 0.4, $p>0.05$ in the first and second sub-periods), soil temperature was significantly and positively
443 correlated to N_2O emissions ($r_{sm}\geq 0.56$, $p<0.001$) (Figure 8). This indicates if soil moisture is not
444 changed and other factors remain constant, the N_2O emission during the daytime is higher than
445 during the night time. The soil microorganisms were more active during the warmer daytime and
446 produced more N_2O emissions, as pointed out in Maljanen et al. (2002). However, the daytime
447 fluxes were not always higher through the whole season as shown on Figure 7; i.e., the daytime
448 fluxes were not higher during the third and the fourth periods because the soil moisture was a
449 predominant factor ($r_{sm}> 0.4$).
450 As expected, mineral nitrogen availability was an important factor in N_2O emissions. The
451 fertilizer applications before June may have caused higher soil N availabilities and higher N_2O
452 concentrations than after June (Figure 6). The fertilizer amount of the second application was

more than twice that of the first application; it most likely contributed to the dramatic increase in N_2O concentration and flux after the second application (Figure 5).

4.4 Response of N_2O emission to precipitation

Soil moisture was strongly dependent on precipitation events. For most precipitation events during the experimental period, the sonic anemometer sensor heads were wet and could not measure the instantaneous wind velocities precisely. Consequently, estimates of the reaction time of emissions to precipitation are lacking. However, there were two events with low rainfall amounts (< 5 mm for each 30-min measurement period) when the sensor heads were not affected (the diagnostic record from the datalogger showed the instruments functioned normally). During these events, the N_2O emissions increased within 30 minutes after rainfall, indicating soil N_2O emission likely responds to rainfall and a change of soil moisture very quickly, as noted previously by Phillips, et al. (2013) using dynamic chambers. Large emissions immediately after rain events have been shown in emission studies of other gases and vapors, for example, Mercury (Bash and Miller, 2009; Gillis and Miller, 2000), and have been attributed to the evacuation of high concentration gas in soil pores as they fill up with water. The same mechanism may be occurring here. In any case, further examination is necessary because the spikes are large and significant emissions during active rainfall may be missed in this and most other field studies.

4.5 Uncertainty in the gap-filling

The gap-filling method used in this study may bring uncertainty to the total N_2O flux estimating. However, it is a common practice that regression model is developed using "good" data (with $u_* \geq$ a threshold value); then the regression model is used to gap-fill the missing data and estimate the total value.

We evaluated the uncertainty of the regression equations used in the gap-fillings by comparing the regressed and the measured flux data when ($u_* \geq 0.2$ m s^{-1}) and found the average error ratio was 14%. The regression equations were from the "good" eddy-covariance data($u_* \geq 0.2$ m s^{-1}). The "good" data may have been overestimated about 12-16% (Table 2). Therefore, the total N_2O may be overestimated from the gap-filling by about 27% to 32% [e.g., 27%=(1+14%)(1+12%)-1].

Based on the equation on Figure 11, the seasonal released N_2O should be 3.76 kg N_2O-N Ha^{-1}. However, from this study, it was 6.87 kg N_2O-N Ha^{-1}. Therefore, the gap-filling and the EC measurement uncertainties may have partially contributed to the overestimated N_2O release.

5. CONCLUSIONS

A new N_2O analyzer (quantum cascade laser spectrometer, model CW-QC-TILDAS-76-CS, Aerodyne Research Inc., Billerica, MA) was operated continuously for EC flux measurements of N_2O in a cornfield in Nolensville, TN during the period of April 4–August 8, 2012. Based on Allan Variance analysis, the precision of the instrument was 0.066 ppbv for 10 Hz measurements. The seasonal mean detection limit of the N_2O flux measurements was 7.56 ug N_2O-N m^{-2} hr^{-1}. The mean frequency loss ratio of the flux measurements was between 0.02 to 0.04 under the conditions of 0.4 m $s^{-1} > u_* \geq 0.2$ m s^{-1} during the day and 0.42 under the conditions of 0.3 m $s^{-1} > u_* \geq 0.2$ m s^{-1}during the night. We conclude that this N_2O EC system can be used to provide reliable N_2O flux measurements.

497 The cumulative N_2O emission from the experimental site during the entire growing season
498 was 6.87 kg N_2O-N ha^{-1}. This study showed that in addition to N availability in soil, the seasonal
499 and diurnal N_2O emission was highly dependent on soil moisture, and extremely high fluxes
500 appeared after an N fertilization event combined with precipitation. Soil moisture variation was a
501 dominant factor affecting N_2O emissions compared to soil temperature.

502 Combining these results with 9 previous studies in the literature allowed some preliminary
503 synthesization. It appears that approximately 1.43% of each unit of N fertilizer was emitted to the
504 atmosphere as N_2O.

505

506 **6. FUTURE RESEARCH**

507 We recommend that future studies focus on developing precision methods of minimizing N_2O
508 emissions by careful spatial and temporal control of fertilization amounts, water availability, and
509 tilling practices. These should include "mechanism" studies quantifying the N_2O flux rates from
510 various interactions of water and N levels in soils. The effects of reducing the episodic nature of
511 fertilization and water availability should be quantified and methods developed to make such
512 reductions. Complete field-scale experiments designed to test application rates and application
513 timing and yields will likely produce more usable results than even complete monitoring of
514 commercial field operations.

515

516

517 **ACKNOWLEDGMENTS**

The authors gratefully acknowledge financial support for this research from USDA- Capacity Building Grant (2011-38821-30971), Evans-Allen grant, and the support from the Illinois State Water Survey at the University of Illinois at Urbana-Champaign. The authors thank Dr. Roger Sauve (Tennessee State University) for helping arrange the commercial farm for the experiment. We also thank Eddie Williams, Daniel Doss, and Emeka Nwaneri for field experimental assistance. Opinions expressed are those of the authors and not necessarily those of the Illinois State Water Survey, the Prairie Research Institute, or the University of Illinois.

REFERENCES

Arnold, K., Nilsson, M., Hanell, B., Weslien, P., and Klemedtsson, L.: Fluxes of CO_2, CH_4 and N_2O from drained organic soils in deciduous forests, Soil Biol. Biochem., 37, 1059–1071, 2005.

Aubinet, M., Grelle, A., Ibrom, A., Rannik, Ü., Moncrieff, J., Foken, T., Kowalski, A. S., Martin, P. H., Berbigier, P., Bernhofer, C., Clement, R., Elbers, J., Granier, A., Grünwald, T., Morgenstern, K., Pilegaard, K., Rebmann, C., Snijders, W., Valentini, R., and Vesala, T.: Estimates of the annual net carbon and water exchange of European forests: the EUROFLUX methodology, Adv. Ecol. Res., 30, 113–173, 2000.

Barr, A.G., A.D. Richardson, D.Y. Hollinger, D. Papale, M.A. Arain, T.A. Black, G. Bohrer, D. Dragoni, M.L. Fischer, L. Gu, B.E. Law, H.A. Margolis, J.H. McCaughey, J.W. Munger, W. Oechel, and K. Schaeffer. 2013. Use of change-point detection for friction-velocity threshold evaluation in eddy-covariance studies. Agricultural and Forest Meteorology, 171-172: 31-45. doi: 10.1016/j.agrformet.2012.11.023.

Bash, J. O. and Miller, D. R.: Growing season total gaseous mercury (TGM) flux measurements over an acer rubrum forest, Atmos. Environ., 43, 5953–5961, 2009.

Bouwman, A. F.: Direct emission of nitrous oxide from agricultural soils, Nutr. Cycl. Agroecosys., 46, 53–70, 1996.

Bouwman, A. F, Boumans, L., and Batjes, N. H.: Emissions of N_2O and NO from fertilized fields: summary of available measurement data, Global Biogeochem. Cy., 16, 1–13, 2002.

Davidson, E. A.: Fluxes of nitrous oxide and nitric oxide from terrestrial ecosystems, in: Microbial production and consumption of greenhouse gases: methane, nitrogen oxides, and halomethanes, American Society for Microbiology, Washington, DC, 219–235, 1991

Davidson, E. A. and Swank, W. T.: Environmental parameters regulating gaseous nitrogen losses from two forested ecosystems via nitrification and denitrification, Appl. Environ. Microb., 52, 1287–1292, 1986.

559 Denmead, O. T.: Approaches to measuring fluxes of methane and nitrous oxide between landscapes
560 and the atmosphere, Plant Soil, 309, 5–24, 2008.
561
562 Di Marco, C. D., Skiba, U., Weston, K., Hargreaves, K., and Fowler, D.: Field scale N_2O flux measurements
563 from grassland using eddy covariance, Water Air Soil Poll., 4, 143–149, 2004.
564
565 Dinsmore, K. J., Skiba, U. M., Billett, M. F., Rees, R. M., and Drewer, J.: Spatial and temporal
566 variability in CH_4 and N_2O fluxes from a Scottish ombrotrophic peatland: implications for
567 modelling and up-scaling, Soil Biol. Biochem., 6, 1315–1323, 2009.
568
569 Dobbie, K. E. and Smith, K. A.: Nitrous oxide emission factors for agricultural soils in Great
570 Britain: the impact of soil water-filled pore space and other controlling variables, Glob.
571 Change Biol., 9, 204–218, 2003.
572
573 Eddypro Version 3.0: Eddypro Version 3.0 User's Guide &, LI-COR, Inc., Lincoln, NE 68504-
574 0425, 2012.
575
576 Edwards, G. C., Thurtell, G. W., Kidd, G. E., Dias, G. M., and Wagner-Riddle, C.: A diode laser
577 based gas monitor suitable for measurement of trace gas exchange using micrometeorological
578 technique, Agr. Forest Meteorol., 115, 71–89, 2003.
579
580 Eugster,W., Zeyer, K., Zeeman, M., Michna, P., Zingg, A., Buchmann, N., and Emmenegger, L.:
581 Methodical study of nitrous oxide eddy covariance measurements using quantum cascade
582 laser spectrometery over a Swiss forest, Biogeosciences, 4, 927–939, doi:10.5194/bg-4-927-
583 2007, 2007.
584
585 Famulari, D., Nemitz, E., Marco, C. D., Phillips, G. J., Thomas, R., House, E., and Fowler, D.:
586 Eddy-covariance measurements of nitrous oxide fluxes above a city, Agr. Forest Meteorol.,
587 150, 786–793, 2010.
588
589 Ferrara, R. M., Loubet, B., Tommasi, P. D., Bertolini, T., Magliulo, V., Cellier, P., Eugster, W., and
590 Rana, G.: Eddy covariance measurement of ammonia fluxes: comparison of high frequency
591 correction methodologies, Agr. Forest Meteorol., 158–159, 30–42, 2012.
592
593 Forster, P., Ramaswamy, V., Artaxo, P., Berntsen, T., Betts, R., Fahey, D. W., Haywood, J., Lean,
594 J., Lowe, D. C., Myhre, G., Nganga, J., Prinn, R., Raga, G., Schulz, M., and Van Dorland, R.:
595 Changes in atmospheric constituents and in radiative forcing, in: Climate Change 2007: The
596 Physical Science Basis. Contribution of Working Group I to the Fourth Assessment Report of
597 the 5 Intergovernmental Panel on Climate Change, Cambridge University Press, Cambridge,
598 Chapt. 2, 2007.
599
600 Gillis, A. A. and Miller, D. R.: Some local environmental effects on mercury emission and absorption
601 at a soil surface, Sci. Total Environ., 260, 191–200, 2000.
602
603 Grant, R. F. and Pattey, E.: Modelling variability in N_2O emissions from fertilized agricultural
604 fields, Soil Biol. Biochem., 35, 225–243, 2003.
605
606 Gu, L., Falge, E. M., Boden, T., Baldocchi, D. D., and Black, T. A.: Objective threshold determination
607 for nighttime eddy flux filtering, Agr. Forest Meteorol., 128, 179–197, 2005.
608
609 Halvorson, A. D., Schweissing, F. C., Bartolo, M. E., and Reule, C. A.: Corn response to nitrogen
610 fertilization in a soil with high residual nitrogen, Agron. J., 97, 1222–1229, 2005.
611
612 Horst, T.W. and Lenschow, D. H.: Attenuation of scalar fluxes measured with spatially-displaced
613 sensors, Bound.-Lay. Meteorol., 130, 275–300, 2009.
614

615 Ibrom, A., Dellwik, E., Larse, S. E., and Pilegaard, K.: On the use of the Webb–Pearman–
616 Leuning theory for closed-path eddy correlation measurements, Tellus B, 59, 937–946, 2007.
617
618 Jones, S. K., Famulari, D., Di Marco, C. F., Nemitz, E., Skiba, U. M., Rees, R. M.,
619 and Sutton, M. A.: Nitrous oxide emissions from managed grassland: a comparison of
620 eddy covariance and static chamber measurements, Atmos. Meas. Tech., 4, 2179–2194,
621 doi:10.5194/amt-4-2179-2011, 2011.
622
623 Jungkunst, H. F., Fless, H., Scherber, C., and Fiedler, S.: Groundwater level controls CO_2, N_2O
624 and CH_4 fluxes of three different hydromorphic soil types of a temperate forest ecosystem,
625 Soil Biol. Biochem., 40, 2047–2057, 2008.
626 Kaimal, J. C. and Finnigan, J. J.: Atmospheric Boundary Layer Flows, 2nd edn., Oxford University
627 Press, New York, 1994.
628
629 Kaimal, J. C., Wyngaard, J. C., Izumi, Y., and Cote, O. R.: Deriving power spectra from a threecomponent
630 sonic anemometer, J. Appl. Meteorol., 7, 827–837, 1972.
631
632 Kitzler, B., Zechmeister-Boltenstern, S., Holtermann, C., Skiba, U., and Butterbach-Bahl, K.:
633 Controls over N_2O, NO_x and CO_2 fluxes in a calcareous mountain forest soil, Biogeosciences,
634 3, 383–395, doi:10.5194/bg-3-383-2006, 2006.
635
636 Klemedtsson, L., Klemedtsson, A. K., Moldan, F., and Weslien, P.: Nitrous oxide emission from
637 Swedish forest soils in relation to liming and simulated increased N-deposition, Biol. Fert.
638 Soils, 25, 290–295, 1996.
639
640 Kroeze, C., Mosier, A., and Bouwman, L.: Closing the global warming budget: a retrospective
641 analysis 1500–1994, Global Biogeochem. Cy., 13, 1–8, 1999.
642
643 Kroon, P. S., Hensen, A., Jonker, H. J. J., Zahniser, M. S., van't Veen, W. H., and Vermeulen,
644 A. T.: Suitability of quantum cascade laser spectroscopy for CH_4 and N_2O eddy
645 covariance flux measurements, Biogeosciences, 4, 715–728, doi:10.5194/bg-4-715-2007,
646 2007.
647
648 Laville, P., Jambert, C., Cellier, P., and Delmas, R.: Nitrous oxide fluxes from a fertilized maize
649 crop using micrometeorological and chamber methods, Agr. Forest Meteorol., 96, 19–38,
650 1999.
651
652 Lee, J., Hopmans, J. W., Kessel., C., King, A. P., Evatt., K. J., Louie, D., Rolston, D. E., and
653 Six, J.: Tillage and seasonal emissions of CO_2, N_2O and NO across a seed bed and at the
654 field scale in a Mediterranean climate, Agr. Ecosyst. Environ., 129, 378–390, 2009.
655
656 Li, J., Tong, X., Yu, Q., Dong, Y., and Peng, C.: Micrometeorological measurements of nitrous
657 oxide exchange in a cropland, Atmos. Environ., 42, 6992–7001, 2008.
658
659 Liu, C., Wang, K., and Zheng, X.: Responses of N_2O and CH_4 fluxes to fertilizer nitrogen addition
660 rates in an irrigated wheat-maize cropping system in northern China, Biogeosciences,
661 9, 839–850, doi:10.5194/bg-9-839-2012, 2012.
662
663 Luo, G. J., Kiese, R.,Wolf, B., and Butterbach-Bahl, K.: Effects of soil temperature and moisture
664 on methane uptake and nitrous oxide emissions across three different ecosystem types,
665 Biogeosciences, 10, 3205–3219, doi:10.5194/bg-10-3205-2013, 2013.
666
667 Ma, B. L.,Wu, T. Y., Tremblay, N., Deen,W., Morrison, M. J., Mclaughlin, N. B., Gregorich, E. G.,
668 and Stewart, G.: Nitrous oxide fluxes from corn fields: on-farm assessment of the amount and
669 timing of nitrogen fertilizer, Glob. Change Biol., 16, 156–170, 2010.
670

Maljanen, M., Martikainen, P. J., Aaltonen, H., and Silvola, J.: Short-term variation in fluxes of carbon dioxide, nitrous oxide and methane in cultivated and forested organic boreal soils, Soil Biol. Biochem., 34, 577–584, 2002.

Mammarella, I.: Lecture 1 EC Method Background and Theory, available at: http://www.abba.ethz.ch/committee/LECTURE_Mammarella.pdf (last access: 31 July 2014), ETH Zurich, Zurich, Switzerland, 2011.

Mammarella, I., Werle, P., Pihlatie, M., Eugster, W., Haapanala, S., Kiese, R., Markkanen, T., Rannik, Ü., and Vesala, T.: A case study of eddy covariance flux of N_2O measured within forest ecosystems: quality control and flux error analysis, Biogeosciences, 7, 427–440, doi:10.5194/bg-7-427-2010, 2010.

Molodovskaya, M., Warland, J., Richards, B. K., Oberg, G., and Steenhuis, T. S.: Nitrous oxide from heterogeneous agricultural landscapes: source contribution analysis by eddy covariance and chambers, Soil Sci. Soc. Am. J., 75, 1829–1838, 2011.

Moncrieff, J., Clement, R., Finnigan, J., and Meyers, T.: Averaging, Detrending, and Filtering of Eddy Covariance Time Series, Vol. 29, Chapt. 2, Kluwer Academic Publishers, Dordrecht, Netherlands, 7–31, 2004.

Mosier, A., C., Kroeze, Nevison, C., Oenema, O., Seitzinger, S., and Cleemput, O.: Closing the global N_2O budget: nitrous oxide emissions through the agricultural nitrogen cy15 cleOECD/IPCC/IEA phase II development of IPCC guidelines for national greenhouse gas inventory methodology, Nutr. Cycl. Agroecosys., 52, 225–248, 1998.

Neftel, A., Flechard, C. R., Ammann, C., Conen, F., Emmenegger, L., and Zeyer, K.: Experimental assessment of N_2O background fluxes in grassland systems, Tellus B, 59, 470–482, 2007.

Neftel, A., Ammann, C., Fischer, C., Spirig, C., Conen, F., Emmenegger, L., Tuzson, B., and Wahlen, S.: N_2O exchange over managed grassland: application of a quantum cascade laser spectrometer for micrometeorological flux measurements, Agr. Forest Meteorol., 150, 775–785, 2010.

Nelson, D.: TDLWintel User's Manual,Aerodyne Research, Inc, Billerica, MA, USA, 2002.

Nelson, D. D., McManus, B., Urbanski, S., Herndon, S., and Zahniser, M. S.: High precision measurements of atmospheric nitrous oxide and methane using thermoelectrically cooled mid-infrared quantum cascade lasers and detectors, Spectrochim. Acta A, 60, 3325–3335, 2004.

Papale, D., Reichstein, M., Aubinet, M., Canfora, E., Bernhofer, C., Kutsch, W., Longdoz, B., Rambal, S., Valentini, R., Vesala, T., and Yakir, D.: Towards a standardized processing of Net Ecosystem Exchange measured with eddy covariance technique: algorithms and uncertainty estimation, Biogeosciences, 3, 571–583, doi:10.5194/bg-3-571-2006, 2006.

Phillips, R. L., Tanaka, D. L., Archer, D. W., and Hanson, J. D.: Fertilizer application timing influences greenhouse gas fluxes over a growing season, J. Environ. Qual., 28, 1569–1579, 2009.

Phillips, R., Griffith, D. W. T., Dijkstra, F.,Lugg, G., Lawrie, R., and Macdonald, B.: Tracking short-term effects 5 of 15N addition on N_2O fluxes using FTIR spectroscopy. J. Environ. Qual. 42, 1327–1340, 2013.

Pihlatie, M., Rinne, J., Ambus, P., Pilegaard, K., Dorsey, J. R., Rannik, Ü., Markkanen, T., Launiainen, S., and Vesala, T.: Nitrous oxide emissions from a beech forest floor measured by eddy covariance and soil enclosure techniques, Biogeosciences, 2, 377–387, doi:10.5194/bg-2-377-2005, 2005.

Ravishankara, A. R., Daniel, J. S., and Portmann, R. W.: Nitrous oxide (N_2O): the dominant ozone-depleting substance emitted in the 21st century, Science, 326, 123–125, 2009.

Saleska, S. R., Miller, S. D., Matross, D. M., Goulden, M. L.,Wofsy, S. C., da Rocha, H. R., de Camargo, P. B., Crill, P., Daube, B. C., de Freitas, H. C., Hutyra, L., Keller, M., Kirchhoff, V., Menton, M., Munger, J. W., Pyle, E. H., Rice, A. H., and Silva, H.: Carbon in Amazon forests: unexpected seasonal fluxes and disturbance-induced losses, Science, 302, 1554–1557, 2003.

Schindlbacher, A., Zechmeister-Boltenstern, S., and Butterbach-Bahl, K.: Effects of soil moisture and temperature on NO, NO_2, and N_2O emissions from European forest soils, J. Geophys. Res., 109, D17302, doi:10.1029/2004JD004590, 2004.

Simpson, I. J., Edwards, G. C., Thurtell, G. W., den Hartog, G., Neumann, H. H., and Staebler, R. M.: Micrometeorological measurements of methane and nitrous oxide exchange above a boreal aspen forest, J. Geophys. Res., 102, 29331–29341, 1997.

Smith, K. A., Ball, T., Conen, F., Dobbie, K. E., Massheder, J., and Rey, A.: Exchange of greenhouse gases between soil and atmosphere: interactions of soil physical factors and biological processes, Eur. J. Soil Sci., 54, 779–791, 2003.

Stull, R. B.: An Introduction to Boundary Layer Meteorology, Kluwer Academic Publishers, Dordrecht, 1988.

Tao, L., Sun, K., Buglione, J., and Zondlo, M.: Flux chamber measurements of nitrous oxide emission at Wetlands, available at: http://meri.njmeadowlands.gov/projects/flux-chamber-measurements-of-nitrous-oxide-emission-at-wetlands/ (last access: 31 July 2014), Meadowlands Environmental Research Institute, Lyndhurst, New Jersey, 2013.

Ussiri, D. A. N., Lal, R., and Jarecki, M. K.: Nitrous oxide and methane emissions from longterm tillage under a continuous corn cropping system in Ohio, Soil Till. Res., 104, 247–255, 2009.

Vickers, D. and Mahrt, L.: Quality control and flux sampling problems for tower and aircraft data, J. Atmos Ocean. Tech., 14, 512–526, 1997.

Wagner-Riddle, C., Furon, A., McLaughlin, N. L., Lee, I., Barbeau, J., Jayasundara, S., Parkin, G., Von Bertoldi, P., and Warland, J.: Intensive measurement of nitrous oxide emissions from a corn-soybean-wheat rotation under two contrasting management systems over 5 years, Glob. Change Biol., 8, 1722–1736, 2007.

Wang, K, Zheng, X., Pihlatie, M., Vesala, T., Liu, C., Haapanala, S., Mammarella, I., Rannik, Ü., and Liu, H.: Comparison between static chamber and tunable diode laser-based eddy covariance techniques for measuring nitrous oxide fluxes from a cotton field, Agr. Forest Meteorol., 171–172, 9–19, 2013.

Wienhold, F. G.,Welling, M., and Harris, G.W.: Micrometeorological measurements and source region analysis of nitrous oxide fluxes from an agricultural soil, Atmos. Environ., 29, 2219–2227, 1995.

Zona, D., Janssens, I. A., Verlinden, M. S., Broeckx, L. S., Cools, J., Gioli, B., Zaldei, A., and

Ceulemans, R.: Impact of extreme precipitation and water table change on N_2O fluxes in a bio-energy poplar plantation, Biogeosciences Discuss., 8, 2057–2092, doi:10.5194/bgd-8-2057-2011, 2011.

Zou, J, Huang, Y., Lu, Y., Zheng, X., and Wang, Y.: Direct emission factor for N_2O from rice–winter wheat rotation systems in southeast China, Atmos. Environ., 39, 4755–4765, 2005.

List of Tables

1. Overview of four measurement periods characterized by precipitation and fertilization. Two fertilizer application events were on April 10 and May 14, 2012. Before the experiment, 99 kg N ha^{-1} chicken litter was applied on March 10. Total precipitation was calculated as the sum of precipitation of each period. N/A: not available.

2. Variation of frequency loss ratio $\frac{\Delta ø}{ø}$ and frequency loss correction ratio by EddyPro ($\frac{\Delta ø}{ø}(Eddypro)$) with friction velocity (u^*, m s^{-1}) for May 2012. N/A: not available. Numbers in the cells are mean ± standard deviations.

3. Descriptive statistics for 30-min N_2O concentration and flux for the period of experiment, April 4 - August 8, 2012 ($u_* \geq 0.2$ m s^{-1}). Nonparametric boot-strapping procedure was used to obtain the 95% confidence interval.

4. Statistical results of 30-min soil temperature (°C), soil moisture (%) and N_2O flux (μg N_2O-N m^{-2} hr^{-1}) (mean±95% confidence interval), as well as Pearson correlation coefficients and p value [r(p)] of N_2O flux with soil temperature or soil moisture ($u_* \geq 0.2$ m s^{-1}). N/A: not available.

5. Thirty min N_2O flux (μg N_2O-N m^{-2} hr^{-1}) regression equations with soil moisture (%) and soil temperature (°C) ($u_* \geq 0.2$ m s^{-1}).

6. Summary of N_2O measurements in literature. EC indicates eddy covariance method. `-' indicates data or information is not available directly from the reference.

List of Figures

9. Cumulative N_2O emission for the experimental site, during April 4 to August 8, 2012. Rainfall and N fertilizer applications data were also shown, 24 days before the experiment (March 10) chicken litter was applied at a rate of 99 kg N ha^{-1} (not shown on the figure).

10. Time series of 30-min soil temperature, soil moisture, N_2O concentration, and flux for the whole experimental period. The vertical dashed lines indicate the sub-periods defined in Table 1.

11. Regression of cumulative N_2O emission on the total applied fertilizer N in 10 different studies (where both amount of fertilizer and cumulative N_2O emission are provided) listed in Table 6, the result of this study is indicated by the red square.

Table 1. Overview of four measurement periods characterized by precipitation and fertilization. Two fertilizer application events were on April 10 and May 14, 2012 respectively. Before the experiment 99 kg N ha^{-1} chicken litter was applied on March 10, total precipitation was calculated as the sum of precipitation of each period.

Index	Date	Fertilization kg N ha^{-1}	Total precipitation (mm)
S1D	Apr 4 -- Apr 25, day	39 (URAN-32-0-0)	15.73
S1N	Apr 4 -- Apr 25, night	-	28.68
S2D	Apr 26 -- May 26, day	79 (URAN-32-0-0)	69.82
S2N	Apr 26 -- May 26, night	-	96.23
S3D	May 27 -- Jun 24, day	-	20.32
S3N	May 27 -- Jun 24, night	-	8.62
S4D	Jun 25 -- Aug 8, day	-	74.38
S4N	Jun 25 -- Aug 8, night	-	53.56

877 Table 2. Variation of frequency loss ratio $\frac{\Delta ø}{ø}$ and frequency loss correction ratio by EddyPro $\frac{\Delta \emptyset}{\emptyset}(EP)$

878 with friction velocity (u^*, m s^{-1}) for May 2012. N/A: not available. Numbers in the cells are mean ±

879 standard deviations.

880

u^*	$0 \le u^* < 0.1$			$0.1 \le u^* < 0.2$			$0.2 \le u^* < 0.3$			$0.3 \le u^* < 0.4$			$0.4 \le u^* < 0.5$		
Rang of Loss ratio	≥0	<0	all	≥0	<0	all	≥0	<0	all	≥0	<0	all	≥0	<0	all
Daytime															
# of samples	16	18	34	84	65	149	113	140	253	27	22	49	2	N/A	2
$\frac{\Delta \emptyset}{\emptyset}$	0.43 ±0.48	-0.42 ±0.48	0.02 ±0.64	0.33 ±0.55	-0.45 ±1.10	0.01 ±0.91	0.43 ±1.29	-0.39 ±1.64	0.02 ±1.54	0.22 ±0.22	-0.37 ±0.67	0.04 ±0.55	0.31 ±0.29	N/A	0.31 ±0.29
$\frac{\Delta \emptyset}{\emptyset}(EP)$	0.16 ±0.01	0.16 ±0.01	0.16 ±0.01	0.16 ±0.00	0.15 ±0.00	0.16 ±0.01	0.16 ±0.01	0.16 ±0.01	0.16 ±0.01	0.18 ±0.01	0.17 ±0.01	0.18 ±0.01	0.16 ±0.01	N/A	0.16 ±0.01
Nighttime															
# of samples	145	91	236	47	12	59	4	N/A	4	N/A	N/A	N/A	N/A	N/A	N/A
$\frac{\Delta \emptyset}{\emptyset}$	0.76 ±1.35	-0.84 ±1.66	0.14 ±1.67	0.90 ±1.09	-0.23 ±0.26	0.66 ±1.08	0.42 ±0.27	N/A	0.42 ±0.27	N/A	N/A	N/A	N/A	N/A	N/A
$\frac{\Delta \emptyset}{\emptyset}(EP)$	0.16 ±0.01	0.16 ±0.01	0.16 ±0.01	0.16 ±0.01	0.16 ±0.00	0.16 ±0.01	0.16 ±0.01	N/A	0.16 ±0.01	N/A	N/A	N/A	N/A	N/A	N/A

Table 3. Descriptive statistics for 30-min N_2O concentration and flux for the period of experiment, April 4 - August 8, 2012 ($u_* \geq 0.2$ m s^{-1}). Nonparametric boot-strapping procedure was used to obtain the 95% confidence interval.

	Number of samples	Concentration (ppbv)		Flux (μg N_2O-N m^{-2} hr^{-1})	
		Mean	95% Confidence interval	Mean	95% Confidence interval
Daytime	1224	322.9	±0.2	278.8	±47.5
Nighttime	166	322.5	±0.6	99.9	±29.8
Total	1390	322.8	±0.3	257.5	±42.9

Table 4. Statistical results of 30-min soil temperature (°C), soil moisture (%) and N_2O flux (μg N_2O-N m^{-2} hr^{-1}) (mean ±95% confidence interval), as well as Pearson correlation coefficients and p value [r(p)] of N_2O flux with soil temperature or soil moisture ($u_* \geq 0.2$ m s^{-1}). N/A: not available.

Date	Fertilizer application	Number of samples	Soil temperature	Soil moisture	Flux	Soil temperature r (p)	Soil moisture r(p)
	kg N ha^{-1}		°C	%	μg N_2O-N m^{-2} hr^{-1}		
March 10	99 (chicken litter)	N/A					
Apr 4 -- Apr 25, day	39 (URAN-32-0-0)	274	18.0 ± 0.4	11.8 ±0.3	173.3 ± 27.9	0.18 (0.00)	0.61 (0.00)
Apr 4 -- Apr 25, night		48	18.9 ± 0.6	9.1 ±0.4	62.7 ±20.1	0.45 (0.00)	0.07(0.65)
Apr 26 -- May 26, day	79 (URAN-32-0-0)	392	23.2 ± 0.2	15.0 ±0.4	602.5 ±141.9	-0.20(0.00)	0.49 (0.00)
Apr 26 -- May 26, night		35	21.9 ±0.9	12.0 ±1.1	173.5 ±69.9	0.50 (0.00)	0.64(0.00)
May 27 -- Jun 24, day		326	24.9 ± 0.2	11.1 ± 0.5	60.8 ± 5.6	-0.19(0.00)	0.78 (0.00)
May 27 -- Jun 24, night		36	26.1 ± 0.4	12.0 ±1.7	88.4 ±49.6	0.15 (0.39)	0.61(0.00)
Jun 25 -- Aug 8, day		232	27.1 ± 0.2	10.5 ± 0.5	162.2 ±34.5	-0.25(0.00)	0.57 (0.00)
Jun 25 -- Aug 8, night		47	28.8 ±0.4	8.2 ± 1.1	92.3 ±75.4	-0.49 (0.00)	0.53 (0.00)
Whole experimental period, day		1224	23.2 ±0.2	12.4 ±0.3	279.0 ±48.1	-0.08 (0.00)	0.42 (0.00)
Whole experimental period, night		166	23.9 ±0.7	10.2 ± 0.6	100.1 ± 36.4	0.05 (0.56)	0.50 (0.00)

Table 5. Thirty-min N_2O flux ($\mu g\ N_2O\text{-}N\ m^{-2}\ hr^{-1}$) regression equations ($p<0.01$) with soil moisture (SM, %) and soil temperature (ST, °C) ($u_* \geq 0.2\ m\ s^{-1}$).

Date	Day Equation	R^2	Night Equation	R^2
April 4 - April 25	$20.16e^{19.398SM}$	0.45	-137.74+5.64SM+564.48ST	0.62
April 26 - May 26	$209037600SM^4-11612160SM^3+2360304SM^2-191720SM+66185.28$	0.68	$18e^{16.48SM}$	0.45
May 27 - June 24	$66154.68SM^3-137696.28SM^2+967.68SM+10.08$	0.71	$6.048e^{16.31SM}$	0.70
June 25 - August 8	$20.16e^{18.35SM}$	0.54	$0.5e^{23.11SM}$	0.54

933 Table 6. Summary of N_2O measurements in literature [mean flux (or flux range) and cumulative emission],
934 EC indicates eddy covariance method, '-' indicates data or information is not available directly from the
935 reference.

936

Reference	Location	Period	Plant	Tillage	Fertilizer, kg N ha^{-1}	Method	Flux, μg N_2O-N m^{-2} hr^{-1}	Cumulative emission, kg N_2O-N ha^{-1}
this study	Williamson, USA	04-08.2012	Corn	No till	217	EC	257.5 ±817.7[a]	6.9
Wang et al. (2013)	Shanxi, China	01--10.2009	Cotton	Till	75	Chamber	1.2--468.8	1.43
		01--12.2009	Cotton	Till	75	EC	-10.8—912.0	3.15
Molodovskaya et al. (2011)	Hardford, New York	06--07.2008	Corn	Till	125	Chamber	30.0±48.0	-
			Alfalfa	Till	750	Chamber	66.0±42.0	-
			Between corn and Alfalfa	-	-	EC	78.0±420.0	
Neftel et al. (2010)	central Switzerland	06--09.2008	Grass	Till	230	Chamber	121.0	3.1
						EC	56.5	1.5[b]
Mammarella et al.(2010)	Sorø, Denmark	05.2003	Beech	-	-	Chamber	9.9±0.12[a]	-
						EC	7.2±0.40[a]	-
	Kalevansuo, Finland	04--06.2007	Pine, spruce, birch	-	-	Chamber	4.5±0.03[a]	-
						EC	4.6±1.0[a]	-
Lee et al. (2009)	Yolo, California	04--09.2004	Corn	Standard till	244	Chamber	0- 100.8[b]	3.8
				minimum tillage	244	Chamber	0- 412.0[b]	8.5
Phillips et al. (2009)	Mandan, North Dakota	04--08.2008	Corn	No till	70 (early spring)	Chamber	210.0[c]	0.6±0.31[a]

					70 (late spring)	Chamber	270.0[c]	0.7±0.22[a]
Ussiri et al. (2009)	Clarleston, USA	11.2004-11.2005	Corn	No till	200	Chamber	12.1	0.9
				Chisel till	200	Chamber	30.8	2.0
				Moldboard till	200	Chamber	27.9	1.8
Li et al. (2008)	Luancheng China	1995--1998	Corn		320.5	Gradient	-4410.0—4840.0	-
			Wheat	-	247	Gradient	-2820.0—3590.0	-
Eugster et al. (2007)	Lägeren mountain, Switzerland	10--11.2005	Beech, spruce	-	-	EC	22.4±11.2[a]	-
Kroon et al. (2007)	Reeuwijk, Netherlands	08--11.2006	Grass	-	337	EC	187.2±284.4[a]	-
Wagner-Riddle et al. (2007)	Ontario, Canada	2000--2001	Corn	Till	150	Gradient	24.0[d]	1.2±0.08[a]
				No till	110	Gradient	17.8[d]	1.0±0.07[a]
		2001-2002	Soybean	Till	-	Gradient	15.0[d]	0.7±0.06[a]
				No till	-	Gradient	10.0[d]	0.5±0.01[a]
		2002--2003	Wheat	Till	90	Gradient	17.4[d]	3.0±0.39[a]
				No till	60	Gradient	8.1[d]	0.7 ±0.11[a]
		2003--2004	Corn	Till	150	Gradient	39.1[d]	1.8±0.20[a]
				No till	110	Gradient	10.1[d]	1.6±0.16[a]
		2004--2005	Soybean	Till	-	Gradient	5.9[d]	0.3±0.08[a]
				No till	-	Gradient	3.6[d]	0.3±0.01[a]
Kitzler et al. (2006)	North Tyrol Limestone Alps, Austria	05.2002--04.2003	Spruce, fir, beech	-	-	Chamber	4.5	0.3±0.11[a]
		05.2003--04.2004	Spruce, fir, beech	-	-	Chamber	4.4	0.4±0.09[a]
Zou et al. (2005)	Nanjing, China	05.2002—10.2002	Rice	-	0	Chamber	48.2	1.38±0.01[a]

					150	chamber	100.0[b]	2.67 ±0.07 [a]
					300	chamber	170.0[b]	4.44 ±0.16 [a]
					450	chamber	215.9	6.17 ±0.42 [a]
		11.2002—06.2003	Winter wheat	-	0	chamber	53.8	2.84 ±0.03 [a]
					100	chamber	91.5	4.83 ±0.06 [a]
					200	chamber	110.0[b]	6.44 ±0.08 [a]
					300	chamber	137.8	7.27 ±0.43 [a]
Grant and Pattey (2003)	Ottawa, Canada	05--07.1998	Corn	Till	155	EC	-	2.2
					99	EC	-	1.2
Laville et al. (1999)	Landes de Gascogne, France	06.1999	Corn	Till	200	Chamber	90—990	-
						EC	72—1440	-
Simpson et al. (1997)	Saskatehewan, Canada	04--09.1994	Aspen	-	-	Gradient	5.04 ±2.5	-

937

938 a. Standard deviations.
939 b. Values are not given directly, calculated from known variables.
940 c. The measurements were taken at 10:00-12:00 daily, and used as the daily flux.
941 d. Median, instead of mean.

942

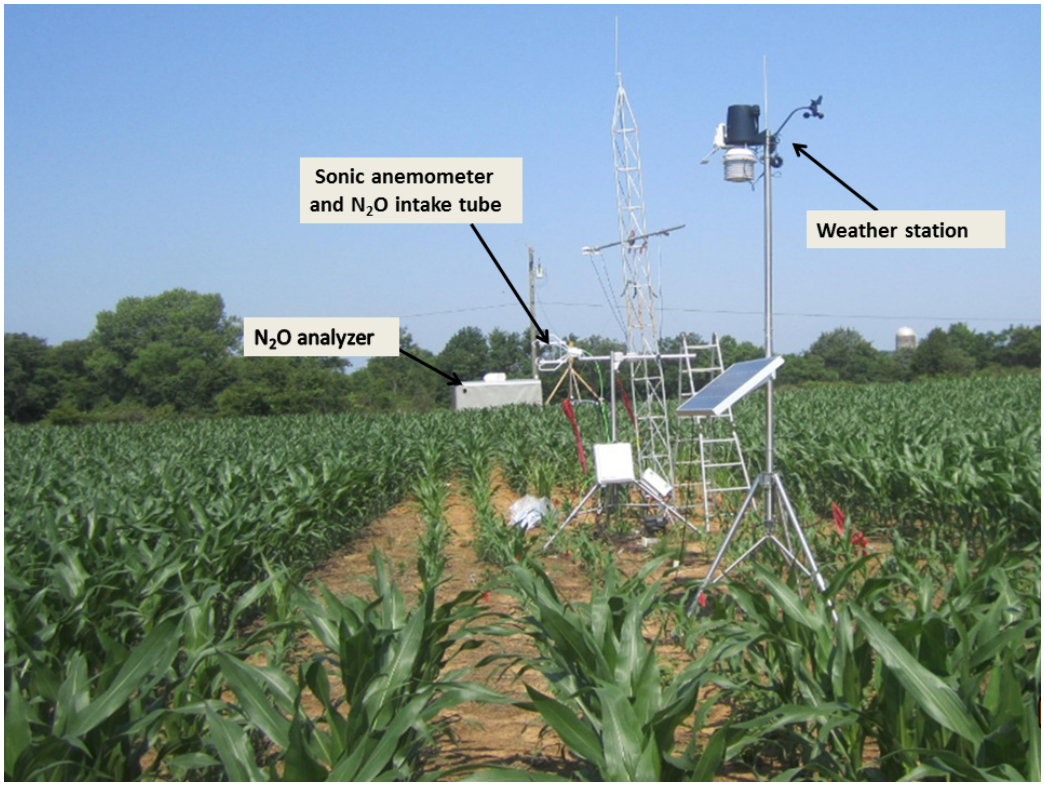

Figure 1: Photo of the experimental site, Williamson County (Nolensville, TN).

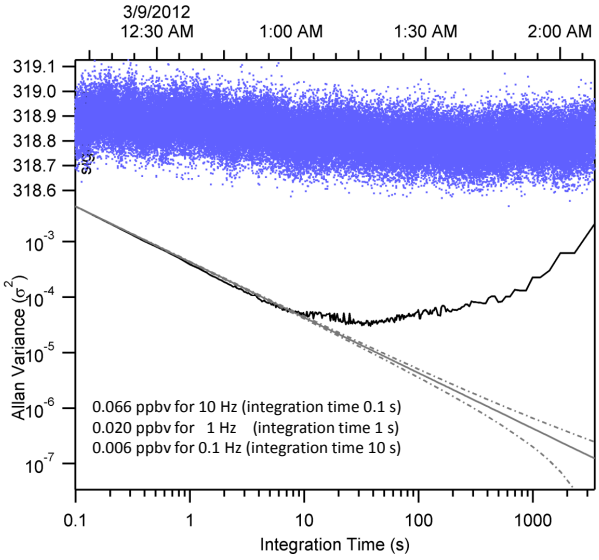

Figure 2: Time series of measured N_2O concentrations (blue dots, ppbv, 10 Hz) under field conditions and the associated Allan variance, downward sloping straight line shows the theoretical behavior of white noise (with a slope of -1, bracketed by dotdash lines showing the 95% confidence interval), provided by Dr. Mark Zahniser at Aerodyn.

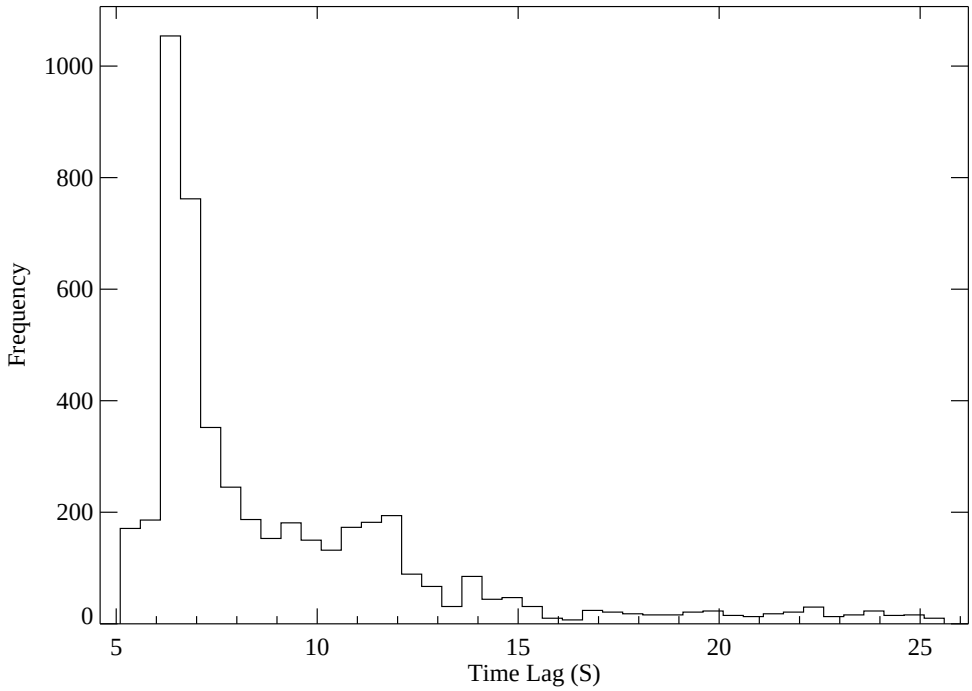

Figure 3: Whole-season histogram of the frequency distribution of time lags of N_2O measurements from wind velocity measurements, found by searching the maximum of cross-covariance.

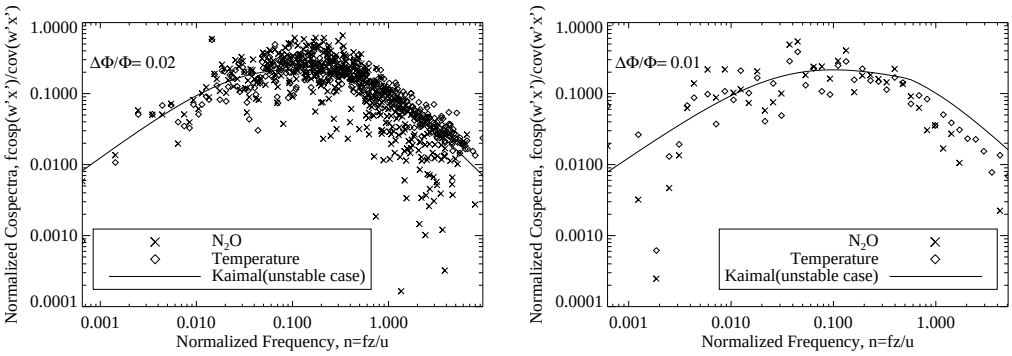

Figure 4: Normalized cospecta, (left) daytime (7 am to 7 pm May 22, 2012, $u_* \geq 0.2$, $L < 0$), (right) night time (7 pm May 16 to 7am May 17, 2012, $u_* \geq 0.2$, $L < 0$). (L is the stability parameter: Monin-Obukhov length (m) output from Eddypro; because under stable conditions ($L > 0$), the eddies may not have been well developed, the nighttime unstable conditions ($L < 0$) were chosen). The axis is normalized frequency, n=fz/u, f is natural frequency (Hz); z is measuring height (m); and u is wind speed (m s^{-1}). The idealized undamped cospectrum according to Kaimal et al. (1972) and sensible heat cospectrum are also given.

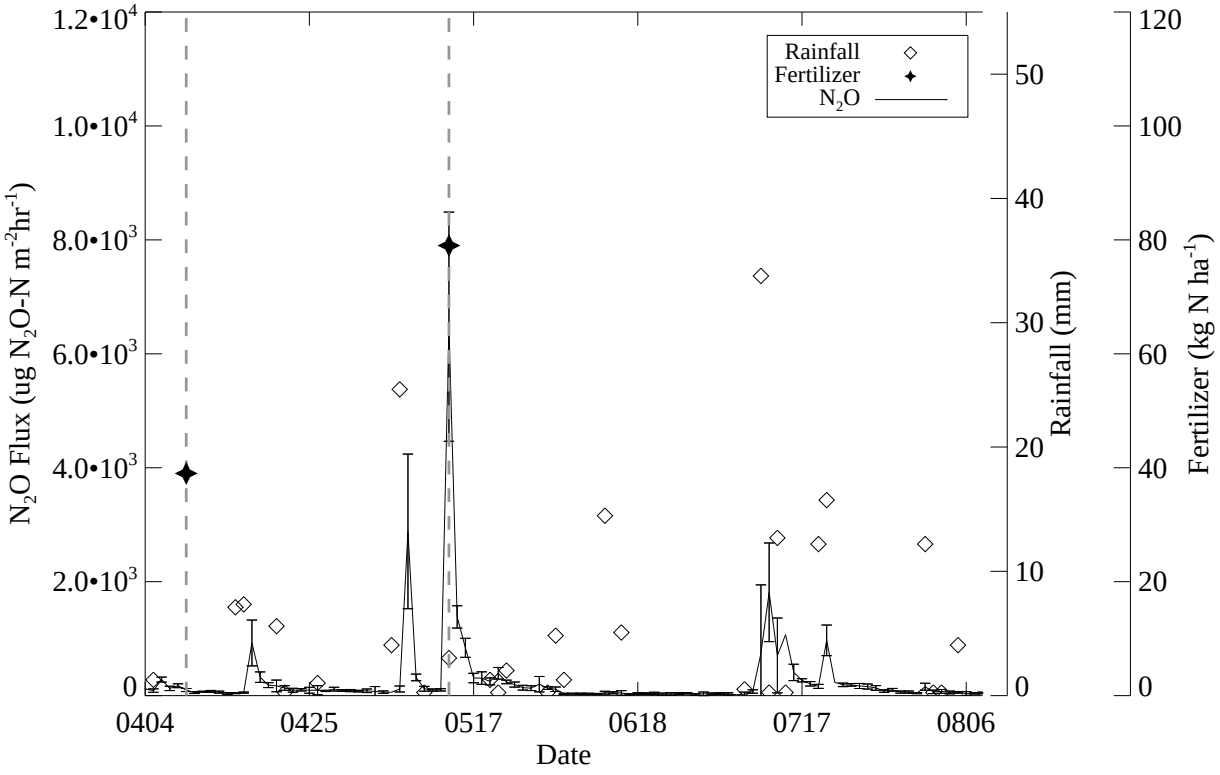

Figure 5: Daily average N_2O flux (μg N_2O-N m^{-2} hr^{-1}) with rainfall and N fertilizer applications from April 4 to August 8, 2012. Error bars were the standard deviations of all data collected on each day ($u_* \geq 0.2$ m s^{-1}), the dates of fertilization were indicated by dashed lines.

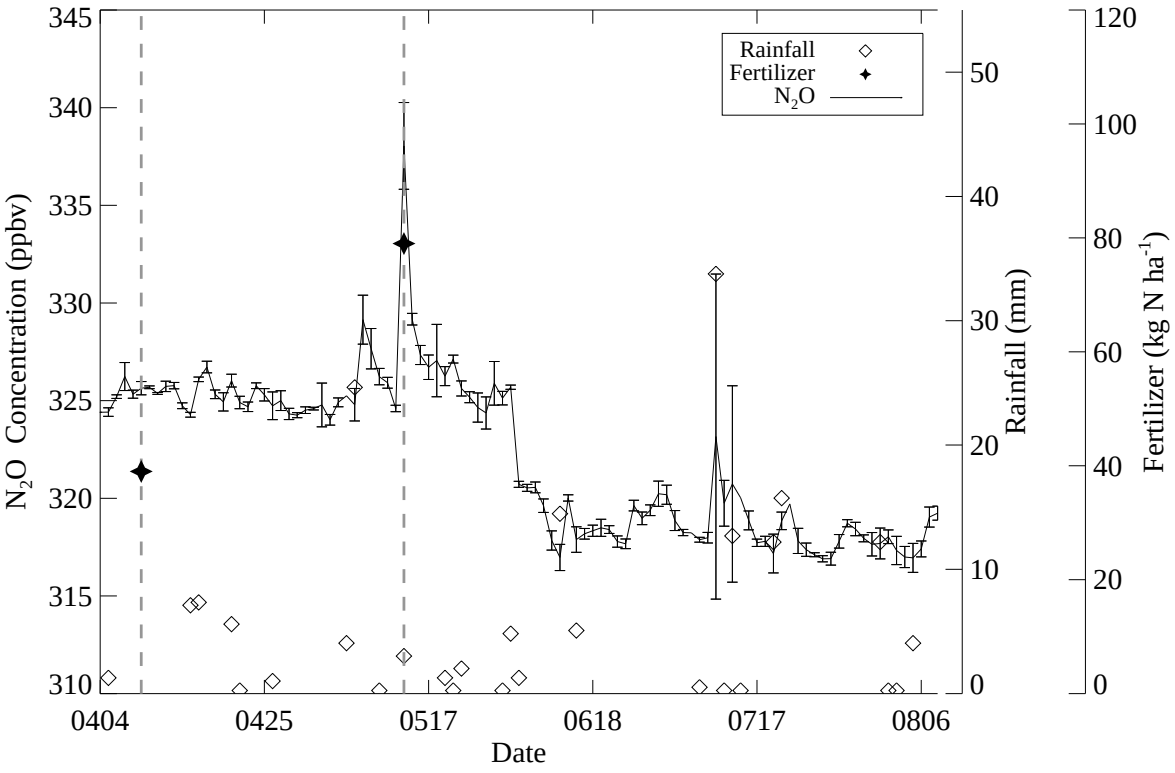

Figure 6: Daily average N_2O concentration (ppbv) with rainfall and N fertilizer applications from April 4 to August 8, 2012. Error bars were the standard deviations of all data collected on each day ($u_* \geq 0.2$ m s^{-1}), the dates of fertilization were indicated by dashed lines.

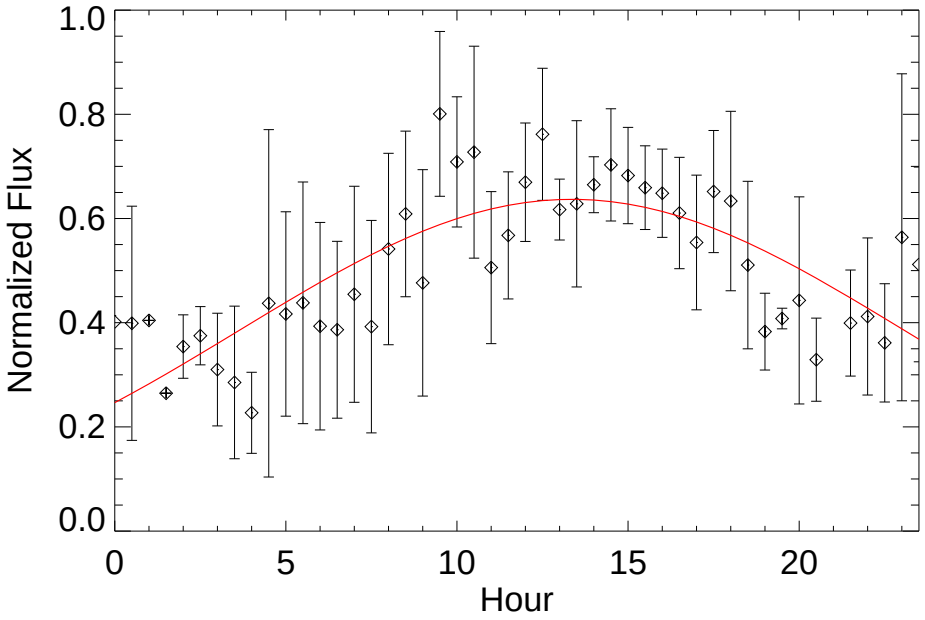

Figure 7: Diurnal variation of 30-min N_2O flux of five selected days when day and night were nearly complete (data points > 20 hours/day and $u_* \geq 0.2$ m s^{-1}). The five days were April 15, April 25, April 26, June 1 and June 10. Bars are 95% confidence interval. Data were normalized by each day maximum.

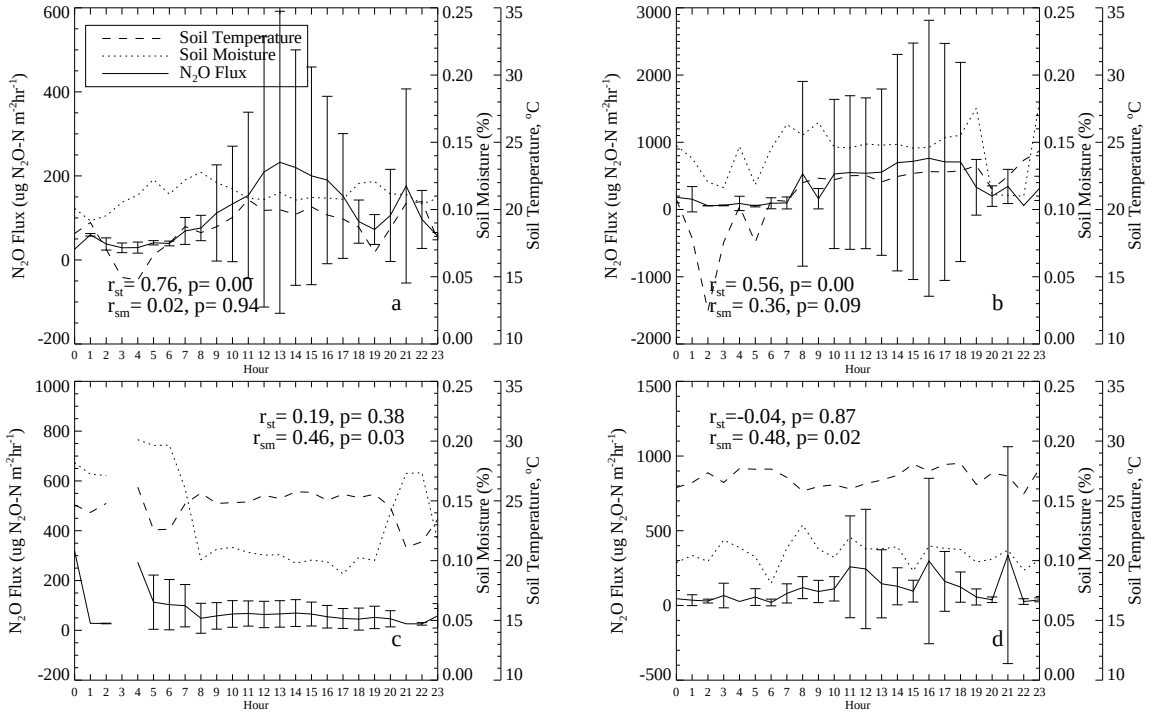

Figure 8: Diurnal variation of 30-min N_2O flux for the four sub-periods defined in Table 1, a. the first period, b. the second period, c. the third period, and d. the fourth period. r_{st} is the correlation coefficient of N_2O flux and soil temperature; r_{sm} is the correlation coefficient of N_2O flux and soil moisture.

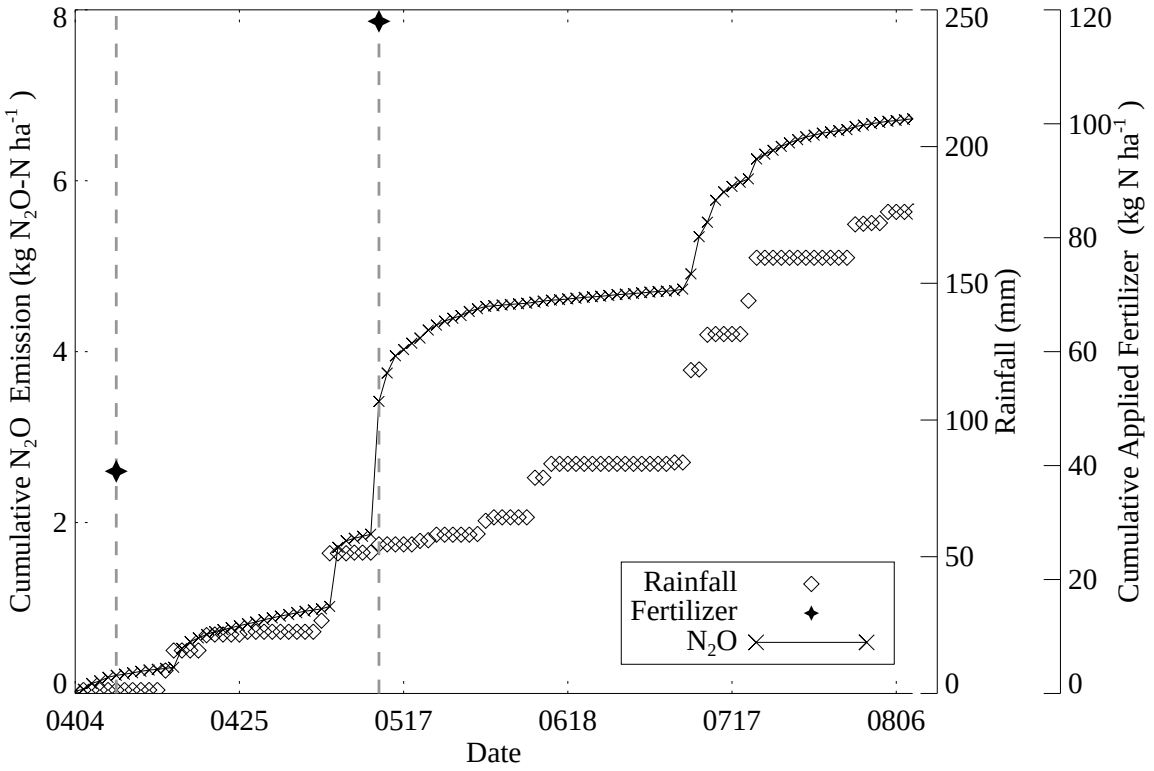

Figure 9: Cumulative N_2O emission for the experimental site, during April 4 to August 8, 2012. Rainfall and N fertilizer applications data were also shown, 24 days before the experiment (March 10) chicken litter was applied at a rate of 99 kg N ha^{-1} (not shown on the figure).

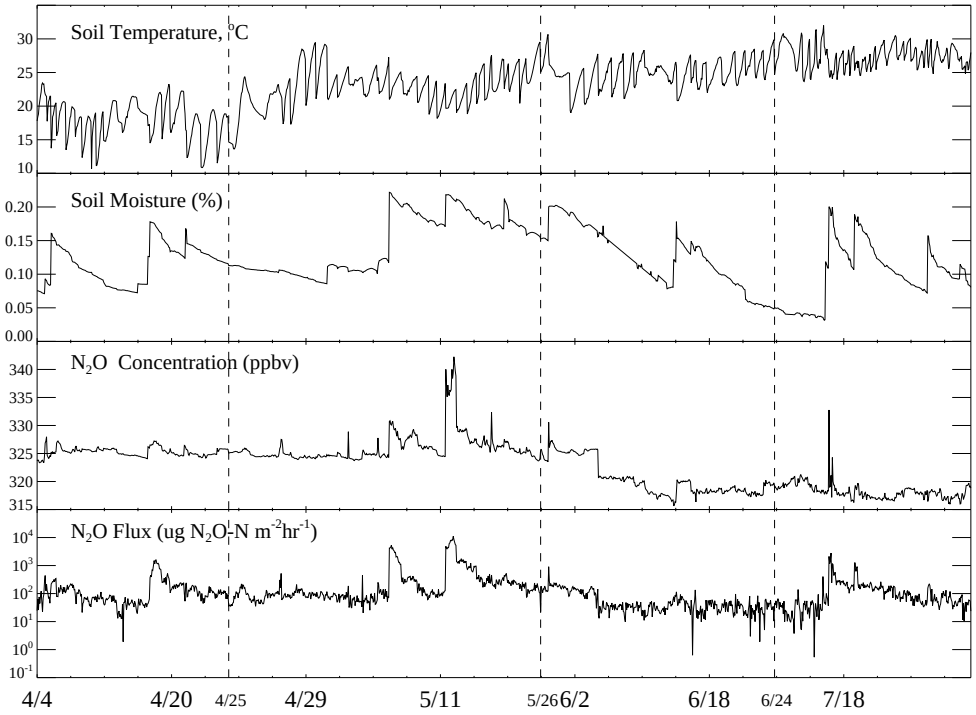

Figure 10: Time series 30-min of soil temperature, soil moisture, N_2O concentration, and flux for the whole experimental period. The vertical dashed lines indicate the sub-periods defined in Table 1.

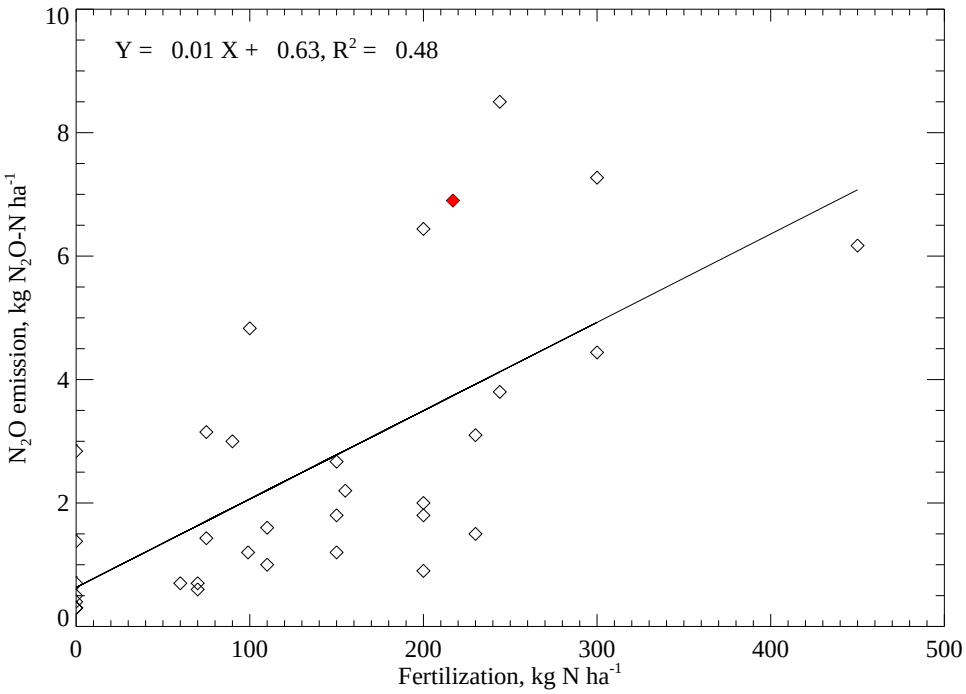

Figure 11: Regression of cumulative N_2O emission on the total applied fertilizer N in 10 different studies (where both amount of fertilizer and cumulative N_2O emission are provided) listed in Table 6, the result of this study is indicated by the red square.